Human umbilical cord mesenchymal stem cells conditioned medium exerts anti-tumor effects on KGN cells in a cell density-dependent manner through activation of the Hippo pathway

Wenjing Wan
Northwest Agriculture University: Northwest Agriculture and Forestry University
Yuyang Miao
Northwest Agriculture University: Northwest Agriculture and Forestry University
Yuwei Niu
Northwest Agriculture University: Northwest Agriculture and Forestry University
Kunyuan Zhu
Northwest Agriculture University: Northwest Agriculture and Forestry University
Yingwan Ma
Northwest Agriculture University: Northwest Agriculture and Forestry University
Menghao Pan
Northwest Agriculture University: Northwest Agriculture and Forestry University
Baohua Ma
Northwest Agriculture University: Northwest Agriculture and Forestry University
Qiang Wei (weiq@nwafu.edu.cn)
Northwest Agriculture University: Northwest Agriculture and Forestry University https://orcid.org/0000-0001-5024-9646

Research Article

Keywords: Human umbilical cord mesenchymal stem cells, conditioned medium, granulosa cell tumor, cell density, contact inhibition, Hippo pathway

Posted Date: August 8th, 2022

DOI: https://doi.org/10.21203/rs.3.rs-1824170/v1

Version of Record: A version of this preprint was published at Stem Cell Research & Therapy on March 20th, 2023. See the published version at https://doi.org/10.1186/s13287-023-03273-z.

Abstract

Objectives

The conditioned medium from human umbilical cord mesenchymal stem cells (UCMSCs-CM) provides a new cell-free therapy for tumors due to its unique secretome. However, there are many contradictory reports about the effect of UCMSCs-CM on tumor cells. The loss of contact inhibition is a common characteristic of tumor cells. A relationship between the effect of UCMSCs-CM on tumor cells and contact inhibition in tumor cells is rarely concerned. Whether the effect of UCMSCs-CM on tumor cells is affected by cell density? Here, we explored the effect of UCMSCs-CM on KGN cell, which is an ovarian granulosa cell tumors cell line, at low or high density.

Materials and Methods

Growth curve and CCK8 assay were used to assess cell proliferation and viability. Scratch wound and matrigel invasion assay were implicated to detect cell motility of KGN cells. UCMSCs-CM effects on cell cycle, apoptosis and pathway-related proteins were investigated by flow cytometry, TUNEL assay, western blot and immunofluorescence analysis respectively.

Results

In growth curve analysis, before KGN cells proliferated into confluence, UCMSCs-CM had no effect on cell proliferation, but once the cells proliferate to contact each other, UCMSCs-CM significantly inhibited proliferation. Meanwhile, when KGN cells were implanted at high density, UCMSCs-CM could induce cell cycle arrest at G1 phase, inhibit cell migration, invasion and promote apoptosis. However, it had no similar effect on KGN cells implanted at low density. In mechanism, the UCMSCs-CM treatment activated the Hippo pathway when KGN cells were implanted at high density. Consistently, the MST1/2 inhibitor, XMU-MP-1, inhibited the activation of the Hippo pathway induced by UCMSCs-CM treatment and accordingly declined the anti-tumor effect of UCMSC-CM on KGN cells.

Conclusion

The effect of UCMSCs-CM on tumor cells is affected by cell density. UCMSCs-CM exerted anti-tumor effect on KGN cells by activating Hippo pathway to restore contact inhibition. Our results suggest that UCMSCs-CM is a promising therapeutic candidate for GCTs treatment.

1. Introduction

Granulosa cell tumor (GCT) is a rare and severe sex cord stromal ovarian tumor, accounting for 5–8% of all ovarian malignancies [1]. GCTs are associated with significant risk of recurrence [2], which is often

nonresponsive to conventional chemotherapies, and 80% of these recurrent cases succumb to their disease [3–5]. To date, there is no standard treatment for patients with recurrent GCT [6].

Umbilical cord mesenchymal stem cells (UCMSCs) are a promising tool in cell therapies due to their multi-potency, self-renewal and immunomodulatory properties [7]. These characteristics endow UCMSCs with potential for application in the novel tumor therapies [8]. In recent years, because of unique secretome and exosomes, the conditioned medium and cell lysate of UCMSCs were used of cell-free tumor therapy [9]. UCMSCs conditioned medium (CM) contains numbers of special exosomes, growth agents, and cytokines. However, the anti-cancer property of UCMSCs-CM remains largely elusive. The human UCMSCs extracts mediated the inhibition of the proliferation of ovarian cancer cells in vitro [10, 11], UCMSCs-CM inhibited the growth of mammary carcinoma, osteosarcoma, bladder cancer, and lymphoma cells in vitro and in vivo [11–13]. Moreover, UCMSCs-CM suppresses breast cancer cells growth and sensitizes cancer cells to radiotherapy through inhibition of the Stat3 signaling pathway [14]. On the other hand, it is reported that UCMSCs-CM promoted the proliferation and migration of Glioblastoma cells, MDA-MB-231 cells, and some subtypes of lung cancer stem cells [15–17]. These contradictory results are usually attributed to the difference in sensibility of various tumor cell types.

The loss of contact inhibition or density-dependent inhibition is one of the key events in oncogenesis [18, 19]. Although there have been many reports about the effect of UCMSCs-CM on tumor cells, a correlation between these effects and contact inhibition on tumor cells is rarely concerned. The Hippo pathway is highly sensitive to cell density and mediate contact inhibition of growth [20, 21]. YAP1 (YES-related protein), as a transcriptional coactivator of pro-proliferation and pro-tumor genes [22, 23], is a main downstream effector of the Hippo pathway [24]. It modulates many of the biological phenotypes of cancer cells, including cell proliferation, invasion and metastasisl [25]. Higher YAP1 expression was significantly associated with poorer overall survival and disease-free survival in adrenocortical carcinoma (ACC), brain lower grade glioma (LGG), and pancreatic adenocarcinoma (PAAD) [26]. Notably, evidence also links the Hippo pathway to GCT with YAP being over-activated, which regulated of GCT cell proliferation and migration [27].

In the present study, we evaluated the effects of the UCMSCs-CM against the granulosa tumour cell line (KGN) at low and high density in vitro. Our study revealed a new mechanism that UCMSCs-CM inhibited the malignant phenotype of KGN cells related to cell density through activating Hippo pathway. The results obtained supported the utility of UCMSCs-CM as a candidate therapeutic agent for GCT.

2. Materials And Methods

2.1 Isolation, culture and identification of hUCMSCs.

Human umbilical cords were obtained from mothers who had given birth at Shaanxi maternal and Child Health Hospital and were used in accordance with the ethical guidelines and accepted human studies protocols at Northwest A&F University. Written informed consent forms were obtained from the healthy umbilical cord donors. HUCMSCs were prepared as previously described [28]. The surface markers

including positive markers CD44, CD29, CD90, and CD105 and negative markers CD34, CD45 of hUCMSCs were analyzed by flow cytometry and CellQuest software (Becton Dickinson). The antibodies against the above surface markers were purchased from BD Biosciences, USA. The induced differentiation of hUCMSCs was conducted in osteogenic (Gibco, A1007201, USA), adipogenic (Gibco, A1007001, USA), or chondrogenic differentiation medium (Gibco, A1007101, USA) according to manufacturer's instructions.

2.2 Cell culture.

Human granulosa-like tumor cell line KGN was obtained from Fenghui Biotechnology (Hunan, China). KGN cells were cultured in DMEM/F12 medium (Hyclone, USA) supplemented with 10% FBS (ExCell Bio, China), 100 IU/mL penicillin and 100 mg/mL streptomycin (Gibco, USA), and incubated at 37°C in a 5% CO_2, 95% humidified atmosphere. For the distinction of high and low density, we followed the previous report [21]. In short, at low-density, cells existed as single cells or small colonies (3×10^3 cells/cm^2). For high-density conditions allows cells to fuse and contact with each other (1.5×10^5 cells/cm^2).

2.3 Harvest of hUCMSC-conditioned medium.

The hUCMSCs at passage 3-6 were cultured in175 cm^2 flask in 20 mL DMEM/F12 supplemented with 10% FBS, Then collected medium every 24 hours until the cell density reached 90% .Subsequently, the conditioned medium collected was filtered through a 0.22 μm syringe filter and Stored at -80 °C until use. Stem cell conditioned media represented as UCMSCs-CM in this study.

2.4 Cell growth curve analysis

For growth curve analysis, cells were seeded in 24 well plates with complete growth medium or UCMSCs-CM at a density of 5×10^3 cells per well. Three well cells from each group were counted with a haemocytometer after 0.05% trypsin digestion every 24h, and then generated a growth curve.

2.5 Cell viability assay

Cell Counting Kit-8 (CCK-8, Abmole, USA) was used to detect the viability of KGN cells. KGN cells were seeded in 96 well plates and cultured for 24 hours. The culture medium was changed to 100μL fresh complete growth medium or UCMSCs-CM and cultured for 48h, added 10 μL CCK8 solutions in each well. The optical density values were measured by microplate reader (Bio-Rad, California, USA) at 450 nm.

2.6 Flow cytometry analysis

Flow cytometry was performed as previously described with some modifications [29, 30]. Apoptosis was detected by using an Annexin V-FITC apoptosis detection kit (BD Biosciences, USA). Cell cycle was detected by propidium iodide (PI) (50 μg/mL) staining. The results were assessed by FACS Aria flow cytometer (BD Biosciences, USA).

2.7 TUNEL assay

TUNEL assay was performed as previously described with some modifications [31]. After be treating with UCMSCs-CM for 48h, the KGN cells were fixed with 4% paraformaldehyde for 30 min at room temperature. According to the TUNEL kit (green fluorescence, C1088, Beyotime, China) manufacturer's instructions, TUNEL test solution was added to the cells devoid of light at 37°C for 60 min, and then the nuclei were finally stained with DAPI (Sigma, USA) for 10 min. Using a fluorescent inverted microscope (Leica, Germany) to obtain the photos.

2.8 Scratch wound assay

The motility of KGN cells was assessed by the scratch wound assay. Cells were plated into a 6-well cell culture plate at a density of 4×10^5 cells/well in complete growth medium and grown to 100% confluence. Using a 200 μL pipette tip to make the straight scratch and washed with PBS twice to remove the cell debris. At 0, 24 and 48 hours after the scratch, images were captured using an optical microscope at x100 magnification after incubation at 37˚C on complete growth medium or UCMSCs-CM.

2.9 Cell invasion assay

The invasion abilities of KGN cells were evaluated by the Matrigel invasion assay. Briefly, KGN cells in 100 μL DMEM/F12 medium containing 10 g/L HSA(CSL Behring, Australian) were plated on each 24-well transwell filter upper chamber (8 μm pore size, Corning, USA) coated with Matrigel(Corning, 356234, USA). And the lower chamber was filled with 500μL complete growth medium or UCMSCs-CM to stimulate cell invasion. After 16 h of incubation, cells on the upper membrane surface were removed from the bottom of the filter, fixed with 4% paraformaldehyde, and stained with 5% crystal violet, 5-8 random fields were captured under an inverted microscope for quantification of each well.

2.10 Western blot analysis

Following previous description, western blot was conducted [32], Primary antibodies specific against cyclin D1 (60186), p27 (25614), Bax (50599), Bcl-2 (12789), β-actin (20536) (all from proteintech, USA), YAP1 (ab52771), p-YAP 1(S127) (ab76252) (all from abcam, UK), LATS1(3477T), p LATS1 (S909) (9157S) (all from Cell Signaling Technology, USA), all the antibodies were used at the concentration 1:1000. Secondary antibody was HRP-labeled donkey anti-mouse/rabbit IgG (H + L) (1:2000) (Proteintech, USA).

2.11 Immunostaining

Immunofluorescence was performed as previously described with some modifications [33]. Cells were fixed in 4% paraformaldehyde and permeabilized with 0.02% Triton X- 100 in PBS, After washing, the cells were blocked with 1% FBS at 25 °C for 20 minutes and then incubated with the primary antibody, rabbit polyclonal anti-YAP antibody (1:200) at 4 °C for 12 hours, after washing, the cells were labeled with a secondary antibody coupled with Aleax-488(1:1000) (Abcam, ab150117, UK) at room temperature for 2

hour. Cells were stained with DAPI (Sigma, USA) at room tempreture for 10 minutes. Then observed under a confocal microscope (Nikon, TiE-A1 plus, Japan).

2.12 Statistical analysis

All data were expressed as the Mean ± SEM from at least three independent experiments. Statistical analysis was carried out by GraphPad Prism 8 software (San Diego, USA). Differences among groups were evaluated by the Student's t test. P-values were calculated, and statistical significance is displayed as *P <0.05, **P <0.01. ***P <0.001, ****P <0.0001, NS: not significant, P>0.05.

3. Results

3.1 Characterization of hUCMSCs

The morphology of the isolated hUCMSCs was a class of polygonal, swirling and fibroblast-like cells under a light microscope (Fig. 1A). The isolated hUCMSCs expressed MSC-related CD surface markers, namely, CD29, CD90, CD44, and CD105. In addition, the hUCMSCs were negative for the hematopoietic markers, including CD34 and CD45 (Fig. 1B). Besides, the isolated hUCMSCs also have differentiation potential into adipocytes, chondrocytes, and osteoblasts (Fig. 1C).

3.2 UCMSCs-CM inhibited the proliferation of KGN cells.

The effect of UCMSCs-CM on the growth of KGN cells was first examined by growth curve analysis. Within 6 days after cell implantated at 5×10^3 cells/well, the cells of the control group and the UCMSCs-CM treatment group proliferated at similar rate. But from the seventh day onwards, at which the cells reached confluence, the cell proliferation in UCMSCs-CM treatment group slowed down significantly, while the cells of the control group continue to proliferate (Fig. 2A). To further characterize the growth inhibitory effects of UCMSCs-CM in confluent cultures of KGN cells, the cellviability of KGN cells treated with UCMSCs-CM for 48 h at low and high density were detected by CCK8 assay. The low density ensures that the contact area between cells is as small as possible, while the high density allows cells contact with each other. The result showed that the cellviability of KGN cells treated with UCMSCs-CM was decreased compared with the control group both at low and high density (Fig. 2B). Meanwhile, the growth and cell morphology of KGN cells was observed. There is a marked difference in the morphologic appearance of control and UCMSCs-CM treated group at high density. Cells in the control group displays a more rounded and small cell shape in dense areas, but cells in the UCMSCs-CM group rest in ellipsoid and larger structure, and cell shrinkage, membrane damage and cell death could be observed. When it at low density, compared with the control group, the density of the UCMSCs-CM group was less dense and the morphologically was altered, but the nuclei were normal and no dead cells were observed (Figure 2C). These data indicated that UCMSCs-CM inhibit the proliferation of KGN cells.

3.3 UCMSCs-CM arrested the cell cycle at the G1 phase of KGN cells at high density.

Flow cytometry was conducted to identify changes in the cell cycle of KGN cells treated with UCMSCs-CM for 48h at low density and high density, the result showed that upon reaching confluence, UCMSCs-CM treated KGN cells underwent a G1 cell cycle arrest (Fig. 3A, B). In order to further explain the G1 arrest in KGN cells in response to the UCMSCs-CM treatments, some cell cycle related proteins were detected by western blot. Compared with the control group, UCMSCs-CM obviously decreased the protein level of cyclin D1 and increased the protein level of p27 in KGN cells at high density (Fig. 3C, D). However, there was no significant difference in the expression levels of these proteins between UCMSCs-CM treatment and no treatment when it at low density. These data indicate that UCMSCs-CM inhibits the cell cycle of KGN cells at the G1 phase at high density rather than at low density.

3.4 UCMSCs-CM induced apoptosis of KGN cells at high density.

The effects of UCMSCs-CM on apoptosis of KGN cells at low and high density were examined. The flow cytometry results presented UCMSCs-CM treatment led to an increase in the proportion of apoptotic cells of KGN cells at high density (10.37±0.6351% vs 3.2±0.5292%, $P < 0.0001$) (Fig. 4A and C). But it had no significant effect at low density (3.3±0.3667% vs 2.6±0.3055%, $P > 0.05$) (Fig. 4A and C). Consistently, in the TUNEL experiment, KGN cells showed a marked increase in emitted green light fluorescence after treatment with UCMSCs-CM at high density than low density (Fig. 4B). Moreover, the levels of pro-apoptotic factors Bax was upregulated, the expression of anti-apoptotic factor Bcl-2 was downregulated and the ratio of Bax/Bcl-2 upregulated significantly in KGN cells treated with UCMSCs-CM at high density. But there was no apparent difference of these protein levels between UCMSCs-CM treatment and no treatment at low density (Fig. 4D, E). Based on these data, UCMSCs-CM could induce KGN cells apoptosis at high density but had no obvious effect when it at low density.

3.5 UCMSCs-CM inhibited the migration and invasion of KGN cells.

The migration of KGN cells treated with UCMSCs-CM was next assessed by performing scratch wound assays. Compared with control group, UCMSCs-CM induced a significant decrease in KGN cell migration after 24 h and 48h, with a reduction of about 15% and about 20% in their migration distance (Fig. 5Aand B). To test the effect of UCMSCs-CM on the capability of KGN cells to invade, invasion assays using matrigel-coated transwells was performed. The result showed that compared with control group, UCMSCs-CM treatment impaired KGN cell invasion as shown by the significant reduction of about 50% in the number of invading cells at high density, but had no effect when it at low density (Fig. 5C and D).

3.6 UCMSCs-CM activated the Hippo-YAP signaling in KGN cells at high density.

Owing to the pivotal role the Hippo pathway plays in GCT development and contact inhibition [20, 27], whether UCMSCs-CM could affect this signaling pathway was examined. KGNs cells with or without treatment of UCMSCs-CM were used to analyze the expression and phosphorylation status of Hippo pathway proteins. Compared with the control group, UCMSCs-CM treatment increased phosphorylation levels of LAST1 (S909), and YAP (S127) in KGN cells at high density (Fig. 6A and C). However, there was

no apparent difference in phosphorylation levels of these proteins between UCMSCs-CM treatment and no treatment at low densities except LAST1 (Fig. 6A and C). To further validate UCMSCs-CM activated the Hippo signaling, KGN cells were pretreated with the MST1/2 inhibitor XMU-MP-1 (5 μM) for 3 h before exposure to UCMSCs-CM. Western blot analysis revealed that XMU-MP-1 effectively inhibited the phosphorylation of LAST1 and YAP induced by UCMSCs-CM (Fig. 6B and D). Since YAP nuclear localization is required for YAP cotranscriptional activity [25, 34-36], YAP localization in KGN cells treated with UCMSCs-CM at low density and high density was observed by confocal microscopy. As expected, when KGN cells were at low density, YAP was preferentially localized in the nucleus regardless of UCMSCs-CM or XMU-MP-1 treatment (Fig. 6E). Oppositely, when KGN cells were at high density, YAP had a dramatic cytoplasmic translocation after treatment with UCMSCs-CM. But when KGN cells were pretreated with XMU-MP-1, YAP still localized in the nucleus even after UCMSCs-CM treatment (Fig. 6E). These results indicated that UCMSCs-CM could activate the Hippo pathway in KGN cells when it at high density.

3.7 UCMSCs-CM suppressed the malignant phenotype of KGN cells depended on activating the Hippo pathway.

Since UCMSCs-CM activated the Hippo pathway in KGN cells at high density, did UCMSCs-CM inhibit the malignant phenotype of KGN cells depend on the Hippo pathway? KGNs were pretreated with XMU-MP-1 before UCMSCs-CM treatment, the results showed that XMU-MP-1 suppressed UCMSCs-CM-induced decline of cell viability (Fig. 7A). Additionally, XMU-MP-1 treatment also ameliorated the changes of the expression levels of Cyclin D1 and p27 induced by UCMSCs-CM (Fig. 7B, C, D). These results indicated that UCMSCs-CM suppresses proliferation of KGN cells through the Hippo signaling pathway. Next, whether UCMSCs-CM-mediated promotion of apoptosis in KGN cells could be reversed by XMU-MP-1 was examined by western blot anaysis, the result revealed that XMU-MP-1 treatment led to a significant reversal of the expression of apoptosis-related proteins including Bax and Bcl-2 induced by UCMSCs-CM (Fig. 7E, F). Furthermore, XMU-MP-1 treatment could rescue KGN cells from UCMSCs-CM-induced invasive inhibition (Fig. 7G, H). These data suggested that the inhibitive effect of UCMSCs-CM on the malignant phenotype of KGN cells was dependent on the activation of the Hippo pathway.

4. Disccusion

GCTs are characterized by ovarian enlargement, excessive estrogenssecretion, long natural history and their tendency to recur years after initial diagnosis [37]. The KGN cell line, which derived from recurrent metastatic GCT, is the only one established cell line, and it is widely used to study GCTs [38].

In recent years, MSCs have become the focus of tumor biotherapy research. However, the tumor-suppressing or tumor-promoting effects of MSCs are still the subject of controversy. The main discrepancies may be due to different types of MSCs from different sources [39, 40]. One of the factors contributing to oncogenesis is that MSCs could transform into tumor-associated fibroblasts(TAF) which plays an important role in tumor development [41]. It has been reported that hUCMSC do not transform to

TAF in breast and ovarian cancer unlike bone marrow mesenchymal stem cells (BMSC) [42]. However, the application of MSCs transplantation is still hindered by many obstacles, including immune compatibility, tumorigenicity, embolism formations [43, 44]. Hence, MSC-conditioned medium, which contains numbers soluble molecules including exosomes and cytokines secreted by MSCs could be used as cell-free tumor therapy [45].

In the current study, before KGN cells proliferated into confluence, UCMSCs-CM had no effect on cell proliferation. But once the cells proliferate to contact each other, UCMSCs-CM significantly inhibited proliferation (Fig. 2A). We hypothesized that UCMSCs-CM inhibited proliferation of KGN cells related to cell density, and UCMSCs-CM might play an anti-tumor role by restoring tumor cell contact inhibition. Then the CCK8 assay was conducted to detect the cell viability and the morphological were observed at the meanwhile. The results showed that UCMSCs-CM decreased the cell viability of KGN cells both at high and low density (Fig. 2B). However, the morphological changes of KGN cells were quite different between high and low density, the cells of the UCMSCs-CM treatment group at high density showed ellipsoid, larger structure, atrophy, and membrane damage(Fig. 2C), similar morphological changes have been previously reported due to the restoration of contact inhibition [46]. When it at low density, the UCMSCs-CM treated cells showed normal nucleus though the morphological changed a lot. It is suggested that the sensitivities of KGN cells with different densities to UCMSCs-CM were different.

More importantly, when KGN cells were implanted at high density, UCMSCs-CM could induce cell cycle arrest at G1 phase, promote apoptosis, and inhibit cell migration and invasion. However, UCMSCs-CM had no similar effect on KGN cells implanted at low density. The cell cycle of contact inhibited cells is often arrested in G1 phase [47], accompanying by the expression level changes of cyclin D1 and p27, which were reported to take part in mediating contact inhibition[48, 49]. In our study, UCMSCs-CM treatment down-regulated the expression of Cyclin D1, up-regulated the expression of p27 in KGN cells when it implanted at high density. In addition, UCMSCs-CM induced the expression of pro-apoptotic factors Bax but inhibited the expression of anti-apoptotic factor Bcl-2 when KGN cells were implanted at high density. It is reported similar promotive effect on apoptosiscell and cycle arrest in human leukemic cell line K562 treated with hUCMSCs and their extracts [50]. Besides, hUCMSC extracts are reported to inhibit ovarian cancer cell lines OVCAR3 and SKOV3 in vitro by inducing cell cycle arrest and apoptosis [11]. Our results consistent with these reports and further confirmed that UCMSCs-CM inhibited proliferation in KGN cells at high density maybe through restoring contact inhibition. Previous studies have shown that MSC-derived exosomes mediate intercellular communication mainly through the exchange of miRNAs [51], and some cell density-dependent miRNA such as miR-590-5p, let − 7a, miR-10b has been reported to inhibited the tumorigenesis by directlly targeting target genes [21, 52]. This study demonstrated that UCMSCs-CM exerts an antitumor effect on KGN cells related to cell density. We speculated that it may some density-related miRNAs carried by exosomes in UCMSC-CM played this role, which warrants further investigation.

Scratch wound and Matrigel invasion assay demonstrated that UCMSCs-CM could strongly inhibit KGN cells migration and invasion (Figs. 5A-D). These data suggest that UCMSCs-CM had the potential to inhibit granulosa cell tumor cell motility which can be helpful to prevent metastasis. It is reported that

suppressive effects of dental pulp stem cells and its conditioned medium on development and migration of colorectal cancer cells through MAPKinase pathway [53], Decidua parietalis mesenchymal stem/stromal cells (DPMSCs) and their secretome inhibit the invasive characteristics of MDA231 cells in vitro [54]. Our results consistent with these studies using MSCs against cancer cell migration and invasion.

The Hippo pathway plays a critical role in the tumorigenesis of human cancer [55]. YAP is regulated by cell density, and its inactivation plays a role in cell contact inhibition [20]. Especially, YAP highly expressed in human GCT tissues, and overexpression of YAP significantly stimulates the proliferation and migration of the GCT cell line [27]. Whether UCMSCs-CM could affect the Hippo pathway in KGN cells was further evaluated. Strikingly, the phosphorylation levels of Hippo signaling proteins LATS1 (S909), and YAP (S127) were all significantly increased and nuclear localization of YAP protein was significantly decreased in the KGN cells after UCMSCs-CM treatment at high density. However, the phosphorylation levels of these proteins were basically unchanged at low density. Moreover, XMU-MP-1, a selective inhibitor of MST1/2, could reverse UCMSCs-CM -induced LATS1 and YAP phosphorylation, resulting in restoring cell viability, rescuing UCMSCs-CM -induced apoptosis, cell cycle related protein changes and invasion inhibition at high density. Collectively, these results implicated that UCMSCs-CM activated the Hippo pathway to inhibit the malignant phenotype when KGN cells reach confluence. There had been similar reports that the Hippo pathway were activated in tumor cells when it at high density [21, 52]. It is reported that ferroptosis has also been found being regulated by the cellular contact and density [56]. Moreover, the YAP/TAZ activation under low density renders cancer cells sensitivity to ferroptosis [57], which may explain why the cell viability decreased and the morphological changed in the UCMSCs-CM treated KGN cells at low density in our study, this speculation needs further investigation.

Conclusions

In conclusion, UCMSCs-CM could significantly inhibit cell viability, cell migration and invasion, induce cell cycle arrest at G1 phase and promote apoptosis of KGN cells at high density through restoration of contact inhibition of KGN cells by activating the Hippo pathway. Our results suggest that UCMSCs-CM is a promising therapeutic candidate for GCTs treatment.

Abbreviations

UCMSCs: Umbilical cord mesenchymalstem cells, CM: conditioned medium, CD markers: Cluster of differentiation markers, GCT : Granulosa cell tumor , KGN: granulosa tumour cell line, YAP: YES-related protein, PBS: Phosphate-buffered solution, DMEM/F12: (Dulbecco's Modified Eagle Media, Nutrient Mixture F-12) (1:1), HSA: Human serm albumin

Declarations

Acknowledgements

Not applicable

Author contributions

WWJ, MYY and NYW performed the experiments. WWJ, ZKY and MYW analyzed data, WWJ, PMH and WQ wrote the manuscript. MBH and WQ designed the experiments. All authors revised the manuscript and approved the final manuscript.

Funding

This work was supported by grants from the National Natural Science Foundation of China (31772818).

Availability of data and materials

The data that support the fndings of this study are available from the corresponding author upon reasonable request.

This study was approved by the Ethics Committee of Northwest A&F University. Written informed consent forms were obtained from the healthy umbilical cord donors.

Consent for publication

Not applicable.

Competing interests

The authors declare that they have no competing interests.

Author details

[1] Key Laboratory of Animal Biotechnology, Ministry of Agriculture, Northwest A&F University, Yangling, Shaanxi, 712100, China. [2] College of Veterinary Medicine, Northwest A&F University, Yangling, Shaanxi, 712100, China.

References

1. S. Jamieson, P.J. Fuller, Molecular pathogenesis of granulosa cell tumors of the ovary, Endocr Rev, 33 (2012) 109-144.
2. K. Miller, W.G. McCluggage, Prognostic factors in ovarian adult granulosa cell tumour, J Clin Pathol, 61 (2008) 881-884.
3. C.M. Annunziata, H.T. Stavnes, L. Kleinberg, A. Berner, L.F. Hernandez, M.J. Birrer, S.M. Steinberg, B. Davidson, E.C. Kohn, Nuclear Factor kappa B Transcription Factors Are Coexpressed and Convey a Poor Outcome in Ovarian Cancer, Cancer, 116 (2010) 3276-3284.

4. S. Jamieson, P.J. Fuller, Molecular Pathogenesis of Granulosa Cell Tumors of the Ovary, Endocr Rev, 33 (2012) 109-144.
5. S. Jamieson, P.J. Fuller, Management of granulosa cell tumour of the ovary, Current Opinion in Oncology, 20 (2008) 560-564.
6. M. Bilandzic, S. Chu, Y. Wang, H.L. Tan, P.J. Fuller, J.K. Findlay, K.L. Stenvers, Betaglycan alters NFkappaB-TGFbeta2 cross talk to reduce survival of human granulosa tumor cells, Mol Endocrinol, 27 (2013) 466-479.
7. M. Mebarki, C. Abadie, J. Larghero, A. Cras, Human umbilical cord-derived mesenchymal stem/stromal cells: a promising candidate for the development of advanced therapy medicinal products, Stem Cell Res Ther, 12 (2021) 152.
8. Y. Yuan, C. Zhou, X. Chen, C. Tao, H. Cheng, X. Lu, Suppression of tumor cell proliferation and migration by human umbilical cord mesenchymal stem cells: A possible role for apoptosis and Wnt signaling, Oncol Lett, 15 (2018) 8536-8544.
9. S. Shin, J. Lee, Y. Kwon, K.S. Park, J.H. Jeong, S.J. Choi, S.I. Bang, J.W. Chang, C. Lee, Comparative Proteomic Analysis of the Mesenchymal Stem Cells Secretome from Adipose, Bone Marrow, Placenta and Wharton's Jelly, Int J Mol Sci, 22 (2021).
10. G. Kalamegam, K.H.W. Sait, N. Anfinan, R. Kadam, F. Ahmed, M. Rasool, M.I. Naseer, P.N. Pushparaj, M. Al-Qahtani, Cytokines secreted by human Wharton's jelly stem cells inhibit the proliferation of ovarian cancer (OVCAR3) cells in vitro, Oncol Lett, 17 (2019) 4521-4531.
11. G. Kalamegam, K.H.W. Sait, F. Ahmed, R. Kadam, P.N. Pushparaj, N. Anfinan, M. Rasool, M.S. Jamal, M. Abu-Elmagd, M. Al-Qahtani, Human Wharton's Jelly Stem Cell (hWJSC) Extracts Inhibit Ovarian Cancer Cell Lines OVCAR3 and SKOV3 in vitro by Inducing Cell Cycle Arrest and Apoptosis, Front Oncol, 8 (2018) 592.
12. K. Gauthaman, F.C. Yee, S. Cheyyatraivendran, A. Biswas, M. Choolani, A. Bongso, Human umbilical cord Wharton's jelly stem cell (hWJSC) extracts inhibit cancer cell growth in vitro, J Cell Biochem, 113 (2012) 2027-2039.
13. H.D. Lin, C.Y. Fong, A. Biswas, M. Choolani, A. Bongso, Human Wharton's jelly stem cells, its conditioned medium and cell-free lysate inhibit the growth of human lymphoma cells, Stem Cell Rev Rep, 10 (2014) 573-586.
14. N. He, Y. Kong, X. Lei, Y. Liu, J. Wang, C. Xu, Y. Wang, L. Du, K. Ji, Q. Wang, Z. Li, Q. Liu, MSCs inhibit tumor progression and enhance radiosensitivity of breast cancer cells by down-regulating Stat3 signaling pathway, Cell Death Dis, 9 (2018) 1026.
15. F. Vulcano, L. Milazzo, C. Ciccarelli, A. Eramo, G. Sette, A. Mauro, G. Macioce, A. Martinelli, R. La Torre, P. Casalbore, H.J. Hassan, A. Giampaolo, Wharton's jelly mesenchymal stromal cells have contrasting effects on proliferation and phenotype of cancer stem cells from different subtypes of lung cancer, Exp Cell Res, 345 (2016) 190-198.
16. P. Li, H. Zhou, G. Di, J. Liu, Y. Liu, Z. Wang, Y. Sun, H. Duan, J. Sun, Mesenchymal stem cell-conditioned medium promotes MDA-MB-231 cell migration and inhibits A549 cell migration by

regulating insulin receptor and human epidermal growth factor receptor 3 phosphorylation, Oncol Lett, 13 (2017) 1581-1586.

17. J. Vieira de Castro, E.D. Gomes, S. Granja, S.I. Anjo, F. Baltazar, B. Manadas, A.J. Salgado, B.M. Costa, Impact of mesenchymal stem cells' secretome on glioblastoma pathophysiology, J Transl Med, 15 (2017) 200.
18. D. Hanahan, R.A. Weinberg, The hallmarks of cancer, Cell, 100 (2000) 57-70.
19. P.J. Nelson, T.O. Daniel, Emerging targets: molecular mechanisms of cell contact-mediated growth control, Kidney Int, 61 (2002) S99-105.
20. B. Zhao, X. Wei, W. Li, R.S. Udan, Q. Yang, J. Kim, J. Xie, T. Ikenoue, J. Yu, L. Li, P. Zheng, K. Ye, A. Chinnaiyan, G. Halder, Z.C. Lai, K.L. Guan, Inactivation of YAP oncoprotein by the Hippo pathway is involved in cell contact inhibition and tissue growth control, Genes Dev, 21 (2007) 2747-2761.
21. M. Mori, R. Triboulet, M. Mohseni, K. Schlegelmilch, K. Shrestha, F.D. Camargo, R.I. Gregory, Hippo signaling regulates microprocessor and links cell-density-dependent miRNA biogenesis to cancer, Cell, 156 (2014) 893-906.
22. B. Zhao, X. Ye, J. Yu, L. Li, W. Li, S. Li, J. Yu, J.D. Lin, C.Y. Wang, A.M. Chinnaiyan, Z.C. Lai, K.L. Guan, TEAD mediates YAP-dependent gene induction and growth control, Genes Dev, 22 (2008) 1962-1971.
23. B. Zhao, K. Tumaneng, K.L. Guan, The Hippo pathway in organ size control, tissue regeneration and stem cell self-renewal, Nat Cell Biol, 13 (2011) 877-883.
24. T. Panciera, L. Azzolin, M. Cordenonsi, S. Piccolo, Mechanobiology of YAP and TAZ in physiology and disease, Nature Reviews Molecular Cell Biology, 18 (2017) 758-770.
25. F.X. Yu, B. Zhao, K.L. Guan, Hippo Pathway in Organ Size Control, Tissue Homeostasis, and Cancer, Cell, 163 (2015) 811-828.
26. B. Wu, X. Tang, H. Ke, Q. Zhou, Z. Zhou, S. Tang, R. Ke, Gene Regulation Network of Prognostic Biomarker YAP1 in Human Cancers: An Integrated Bioinformatics Study, Pathol Oncol Res, 27 (2021) 1609768.
27. D. Fu, X. Lv, G. Hua, C. He, J. Dong, S.M. Lele, D.W. Li, Q. Zhai, J.S. Davis, C. Wang, YAP regulates cell proliferation, migration, and steroidogenesis in adult granulosa cell tumors, Endocr Relat Cancer, 21 (2014) 297-310.
28. L.R. Gao, N.K. Zhang, Q.A. Ding, H.Y. Chen, X. Hu, S. Jiang, T.C. Li, Y. Chen, Z.G. Wang, Y. Ye, Z.M. Zhu, Common expression of stemness molecular markers and early cardiac transcription factors in human Wharton's jelly-derived mesenchymal stem cells and embryonic stem cells, Cell Transplant, 22 (2013) 1883-1900.
29. L. Wang, B. Li, X. Yi, X. Xiao, Q. Zheng, L. Ma, Circ_SMAD4 promotes gastric carcinogenesis by activating wnt/β-catenin pathway, Cell Prolif, 54 (2021) e12981.
30. Y. Miao, W. Wan, K. Zhu, M. Pan, X. Zhao, B. Ma, Q. Wei, Effects of 4-vinylcyclohexene diepoxide on the cell cycle, apoptosis, and steroid hormone secretion of goat ovarian granulosa cells, In Vitro Cell Dev Biol Anim, 58 (2022) 220-231.

31. H. Liu, F. Wang, Y. Zhang, Y. Xing, Q. Wang, Exosomal microRNA-139-5p from mesenchymal stem cells accelerates trophoblast cell invasion and migration by motivation of the ERK/MMP-2 pathway via downregulation of protein tyrosine phosphatase, J Obstet Gynaecol Res, 46 (2020) 2561-2572.
32. F. Fontana, M. Marzagalli, M. Raimondi, V. Zuco, N. Zaffaroni, P. Limonta, δ-Tocotrienol sensitizes and re-sensitizes ovarian cancer cells to cisplatin via induction of G1 phase cell cycle arrest and ROS/MAPK-mediated apoptosis, Cell Prolif, 54 (2021) e13111.
33. Z. Li, M. Zhang, J. Zheng, Y. Tian, H. Zhang, Y. Tan, Q. Li, J. Zhang, X. Huang, Human Umbilical Cord Mesenchymal Stem Cell-Derived Exosomes Improve Ovarian Function and Proliferation of Premature Ovarian Insufficiency by Regulating the Hippo Signaling Pathway, Front Endocrinol (Lausanne), 12 (2021) 711902.
34. F.D. Camargo, S. Gokhale, J.B. Johnnidis, D. Fu, G.W. Bell, R. Jaenisch, T.R. Brummelkamp, YAP1 increases organ size and expands undifferentiated progenitor cells, Curr Biol, 17 (2007) 2054-2060.
35. C. Stein, A.F. Bardet, G. Roma, S. Bergling, I. Clay, A. Ruchti, C. Agarinis, T. Schmelzle, T. Bouwmeester, D. Schübeler, A. Bauer, YAP1 Exerts Its Transcriptional Control via TEAD-Mediated Activation of Enhancers, PLoS Genet, 11 (2015) e1005465.
36. L. Ritchey, T. Ha, A. Otsuka, K. Kabashima, D. Wang, Y. Wang, D.R. Lowy, G. Tosato, DLC1 deficiency and YAP signaling drive endothelial cell contact inhibition of growth and tumorigenesis, Oncogene, 38 (2019) 7046-7059.
37. S. Jamieson, P.J. Fuller, Characterization of the inhibitor of kappaB kinase (IKK) complex in granulosa cell tumors of the ovary and granulosa cell tumor-derived cell lines, Horm Cancer, 4 (2013) 277-292.
38. Y. Nishi, T. Yanase, Y. Mu, K. Oba, I. Ichino, M. Saito, M. Nomura, C. Mukasa, T. Okabe, K. Goto, R. Takayanagi, Y. Kashimura, M. Haji, H. Nawata, Establishment and characterization of a steroidogenic human granulosa-like tumor cell line, KGN, that expresses functional follicle-stimulating hormone receptor, Endocrinology, 142 (2001) 437-445.
39. F. Mosna, L. Sensebé, M. Krampera, Human bone marrow and adipose tissue mesenchymal stem cells: a user's guide, Stem Cells Dev, 19 (2010) 1449-1470.
40. B.J. Jansen, C. Gilissen, H. Roelofs, A. Schaap-Oziemlak, J.A. Veltman, R.A. Raymakers, J.H. Jansen, G. Kögler, C.G. Figdor, R. Torensma, G.J. Adema, Functional differences between mesenchymal stem cell populations are reflected by their transcriptome, Stem Cells Dev, 19 (2010) 481-490.
41. E.L. Spaeth, J.L. Dembinski, A.K. Sasser, K. Watson, A. Klopp, B. Hall, M. Andreeff, F. Marini, Mesenchymal stem cell transition to tumor-associated fibroblasts contributes to fibrovascular network expansion and tumor progression, PLoS One, 4 (2009) e4992.
42. A. Subramanian, G. Shu-Uin, N. Kae-Siang, K. Gauthaman, A. Biswas, M. Choolani, A. Bongso, F. Chui-Yee, Human umbilical cord Wharton's jelly mesenchymal stem cells do not transform to tumor-associated fibroblasts in the presence of breast and ovarian cancer cells unlike bone marrow mesenchymal stem cells, J Cell Biochem, 113 (2012) 1886-1895.

43. W. Zhao, D.G. Phinney, D. Bonnet, M. Dominici, M. Krampera, Mesenchymal stem cell biodistribution, migration, and homing in vivo, Stem Cells Int, 2014 (2014) 292109.
44. A. Putra, I. Rosdiana, D.M. Darlan, I. Alif, F. Hayuningtyas, I. Wijaya, R. Aryanti, F.R. Makarim, A.D. Antari, Intravenous Administration is the Best Route of Mesenchymal Stem Cells Migration in Improving Liver Function Enzyme of Acute Liver Failure, Folia Med (Plovdiv), 62 (2020) 52-58.
45. N.S. Hardiany, E.C. Yo, E. Ngadiono, S.I. Wanandi, Gene Expression of Molecules Regulating Apoptotic Pathways in Glioblastoma Multiforme Treated with Umbilical Cord Stem Cell Conditioned Medium, Malays J Med Sci, 26 (2019) 35-45.
46. J. Schrader, O. Deuster, B. Rinn, M. Schulz, A. Kautz, R. Dodel, B. Meyer, Y. Al-Abed, K. Balakrishnan, J.P. Reese, M. Bacher, Restoration of contact inhibition in human glioblastoma cell lines after MIF knockdown, BMC Cancer, 9 (2009) 464.
47. S.B. Carter, Tissue homeostasis and the biological basis of cancer, Nature, 220 (1968) 970-974.
48. A.A. Chassot, G. Lossaint, L. Turchi, G. Meneguzzi, D. Fisher, G. Ponzio, V. Dulic, Confluence-induced cell cycle exit involves pre-mitotic CDK inhibition by p27(Kip1) and cyclin D1 downregulation, Cell Cycle, 7 (2008) 2038-2046.
49. R.Y. Poon, H. Toyoshima, T. Hunter, Redistribution of the CDK inhibitor p27 between different cyclin.CDK complexes in the mouse fibroblast cell cycle and in cells arrested with lovastatin or ultraviolet irradiation, Mol Biol Cell, 6 (1995) 1197-1213.
50. M.A.H. Huwaikem, G. Kalamegam, G. Alrefaei, F. Ahmed, R. Kadam, T. Qadah, K.H.W. Sait, P.N. Pushparaj, Human Wharton's Jelly Stem Cell Secretions Inhibit Human Leukemic Cell Line K562 in vitro by Inducing Cell Cycle Arrest and Apoptosis, Front Cell Dev Biol, 9 (2021) 614988.
51. S. Rani, A.E. Ryan, M.D. Griffin, T. Ritter, Mesenchymal Stem Cell-derived Extracellular Vesicles: Toward Cell-free Therapeutic Applications, Mol Ther, 23 (2015) 812-823.
52. C. Ou, Z. Sun, X. Li, X. Li, W. Ren, Z. Qin, X. Zhang, W. Yuan, J. Wang, W. Yu, S. Zhang, Q. Peng, Q. Yan, W. Xiong, G. Li, J. Ma, MiR-590-5p, a density-sensitive microRNA, inhibits tumorigenesis by targeting YAP1 in colorectal cancer, Cancer Lett, 399 (2017) 53-63.
53. E. Nikkhah, F. Kalalinia, M. Asgharian Rezaee, Z. Tayarani-Najaran, Suppressive effects of dental pulp stem cells and its conditioned medium on development and migration of colorectal cancer cells through MAPKinase pathways, Iran J Basic Med Sci, 24 (2021) 1292-1300.
54. Y. Basmaeil, E. Bahattab, A. Al Subayyil, H.B. Kulayb, M. Alrodayyan, M. Abumaree, T. Khatlani, Decidua Parietalis Mesenchymal Stem/Stromal Cells and Their Secretome Diminish the Oncogenic Properties of MDA231 Cells In Vitro, Cells, 10 (2021).
55. S. Ma, Z. Meng, R. Chen, K.L. Guan, The Hippo Pathway: Biology and Pathophysiology, Annu Rev Biochem, 88 (2019) 577-604.
56. J. Wu, A.M. Minikes, M. Gao, H. Bian, Y. Li, B.R. Stockwell, Z.N. Chen, X. Jiang, Intercellular interaction dictates cancer cell ferroptosis via NF2-YAP signalling, Nature, 572 (2019) 402-406.
57. T. Sun, J.T. Chi, Regulation of ferroptosis in cancer cells by YAP/TAZ and Hippo pathways: The therapeutic implications, Genes Dis, 8 (2021) 241-249.

ol>

- Bray F, Ferlay J, Soerjomataram I, Siegel RL, Torre LA, Jemal A. Global cancer statistics 2018: GLOBOCAN estimates of incidence and mortality worldwide for 36 cancers in 185 countries. CA: Cancer J Clin. 2018;68(6):394-424.
- Arnold M, Sierra MS, Laversanne M, Soerjomataram I, Jemal A, Bray F. Global patterns and trends in colorectal cancer incidence and mortality. Gut. 2017;66(4):683-91.
- Deng Y, Wei B, Zhai Z, Zheng Y, Yao J, Wang S, et al. Dietary risk related colorectal cancer burden: Estimates from 1990 to 2019. Front Nutr. 2021:568.
- Yang J, McDowell A, Kim EK, Seo H, Lee WH, Moon C-M, et al. Development of a colorectal cancer diagnostic model and dietary risk assessment through gut microbiome analysis. Exp Mol Med. 2019;51(10):1-15.
- Wang Z-q, Zhang L, Zheng H, Guo W-b, Gao Y, Zhao Y-f, et al. Burden and trend of ischemic heart disease and colorectal cancer attributable to a diet low in fiber in China, 1990–2017: findings from the Global Burden of Disease Study 2017. Eur J Nutr. 2021;60(7):3819-27.
- Song M, Chan AT, Sun J. Influence of the gut microbiome, diet, and environment on risk of colorectal cancer. Gastroenterology. 2020;158(2):322-40.
- Wang Z, Zhang L, Guo W, Gao Y, Li X, Zhao Y, et al. Burden of colorectal cancer attributable to diet low in milk in China, 1990–2017: findings from the global burden of disease study 2017. J Hum Nutr Diet. 2021;34(1):233-42.
- Feng Y-L, Shu L, Zheng P-F, Zhang X-Y, Si C-J, Yu X-L, et al. Dietary patterns and colorectal cancer risk: a meta-analysis. Eur J Cancer Prev. 2017;26(3):201-11.
- Forouzanfar MH, Afshin A, Alexander LT, Anderson HR, Bhutta ZA, Biryukov S, et al. Global, regional, and national comparative risk assessment of 79 behavioural, environmental and occupational, and metabolic risks or clusters of risks, 1990–2015: a systematic analysis for the Global Burden of Disease Study 2015. The lancet. 2016;388(10053):1659-724.
- . Annual report of national cancer registration: cancer incidence in 2005 and survival for 1993–2005. Available from: http://www.iarc. fr/ Accessed 2008 Sep 10.
- Safiri S, Sepanlou SG, Ikuta KS, Bisignano C, Salimzadeh H, Delavari A, et al. The global, regional, and national burden of colorectal cancer and its attributable risk factors in 195 countries and territories, 1990–2017: a systematic analysis for the Global Burden of Disease Study 2017. Lancet Gastroenterol Hepatol. 2019;4(12):913-33.
- Lassen AD, Lehmann C, Andersen EW, Werther MN, Thorsen AV, Trolle E, et al. Gender differences in purchase intentions and reasons for meal selection among fast food customers–Opportunities for healthier and more sustainable fast food. Food Qual Prefer. 2016;47:123-9.
- Haslam A, Wagner Robb S, Hébert JR, Huang H, Ebell MH. Association between dietary pattern scores and the prevalence of colorectal adenoma considering population subgroups. Nutr Diet. 2018;75(2):167-75.

- Lee J, Shin A, Choi J-Y, Kang D, Lee J-K. Adherence to the recommended intake of calcium and colorectal cancer risk in the HEXA study. Cancer Rese Treat: Official J Korean Cancer Assoc. 2021;53(1):140.
- Sasso A, Latella G. Dietary components that counteract the increased risk of colorectal cancer related to red meat consumption. Int J Food Sci Nutr. 2018;69(5):536-48.
- Vulcan A, Manjer J, Ericson U, Ohlsson B. Intake of different types of red meat, poultry, and fish and incident colorectal cancer in women and men: results from the Malmö Diet and Cancer Study. Food Nutr Res. 2017.
- Cho Y, Lee J, Oh JH, Chang HJ, Sohn DK, Shin A, et al. Inflammatory dietary pattern, IL-17F genetic variant, and the risk of colorectal cancer. Nutrients. 2018;10(6):724.
- Barrubés L, Babio N, Becerra-Tomás N, Rosique-Esteban N, Salas-Salvadó J. Association between dairy product consumption and colorectal cancer risk in adults: a systematic review and meta-analysis of epidemiologic studies. Adv Nutr. 2019;10(suppl_2):S190-S211.
- Larsson SC, Mason AM, Kar S, Vithayathil M, Carter P, Baron JA, et al. Genetically proxied milk consumption and risk of colorectal, bladder, breast, and prostate cancer: a two-sample Mendelian randomization study. BMC Med. 2020;18(1):1-7.
- Aune D, Chan DS, Lau R, Vieira R, Greenwood DC, Kampman E, et al. Dietary fibre, whole grains, and risk of colorectal cancer: systematic review and dose-response meta-analysis of prospective studies. BMJ. 2011;343.
- Darbandi M, Najafi F, Pasdar Y, Mostafaei S, Rezaeian S. Factors associated with overweight and obesity in adults using structural equation model: mediation effect of physical activity and dietary pattern. Eat Weight Disord. 2020;25(6):1561-71.
- Hsu K-J, Liao C-D, Tsai M-W, Chen C-N. Effects of exercise and nutritional intervention on body composition, metabolic health, and physical performance in adults with sarcopenic obesity: a meta-analysis. Nutrients. 2019;11(9):2163.
- Jessri M, Wolfinger RD, Lou WY, L'Abbé MR. Identification of dietary patterns associated with obesity in a nationally representative survey of Canadian adults: Application of a priori, hybrid, and simplified dietary pattern techniques. Am J Clin Nutr. 2017;105(3):669-84.
- Sun J, Buys NJ, Hills AP. Dietary pattern and its association with the prevalence of obesity, hypertension and other cardiovascular risk factors among Chinese older adults. Int J Environ Res Public Health. 2014;11(4):3956-71.
- Dong Y, Zhou J, Zhu Y, Luo L, He T, Hu H, et al. Abdominal obesity and colorectal cancer risk: systematic review and meta-analysis of prospective studies. Biosci Rep. 2017;37(6).
- Elangovan A, Skeans J, Landsman M, Ali SM, Elangovan AG, Kaelber DC, et al. Colorectal cancer, age, and obesity-related comorbidities: a large database study. Dig Dis Sci. 2021;66(9):3156-63.
- Liu P-H, Wu K, Ng K, Zauber AG, Nguyen LH, Song M, et al. Association of obesity with risk of early-onset colorectal cancer among women. JAMA Oncol. 2019;5(1):37-44.

- Bilski J, Mazur-Bialy A, Wojcik D, Surmiak M, Magierowski M, Sliwowski Z, et al. Role of obesity, mesenteric adipose tissue, and adipokines in inflammatory bowel diseases. Biomolecules. 2019;9(12):780.
- Nani A, Murtaza B, Sayed Khan A, Khan NA, Hichami A. Antioxidant and anti-inflammatory potential of polyphenols contained in Mediterranean diet in obesity: Molecular mechanisms. Molecules. 2021;26(4):985.
- Endo H, Hosono K, Uchiyama T, Sakai E, Sugiyama M, Takahashi H, et al. Leptin acts as a growth factor for colorectal tumours at stages subsequent to tumour initiation in murine colon carcinogenesis. Gut. 2011;60(10):1363-71.
- Modzelewska P, Chludzińska S, Lewko J, Reszeć J. The influence of leptin on the process of carcinogenesis. Contemp Oncol. 2019;23(2):63.
- Engin A. Diet-induced obesity and the mechanism of leptin resistance. Obes Lipot. 2017:381-97.
- Kelesidis I, Kelesidis T, Mantzoros C. Adiponectin and cancer: a systematic review. Br J Cancer. 2006;94(9):1221-5.
- Wei EK, Giovannucci E, Fuchs CS, Willett WC, Mantzoros CS. Low plasma adiponectin levels and risk of colorectal cancer in men: a prospective study. J Natl Cancer Inst. 2005;97(22):1688-94.
- Ellulu MS, Patimah I, Khaza'ai H, Rahmat A, Abed Y. Obesity and inflammation: the linking mechanism and the complications. Arch Med Sci. 2017;13(4):851.
- Wei X, Li X, Kong F, Ma L, Sui Y, Chen D, et al. TNF-α activates Wnt signaling pathway to promote the invasion of human colon cancer stem cells. Xi bao yu fen zi Mian yi xue za zhi= Chin J Cell Mol Immun. 2018;34(11):982-8.

Figures

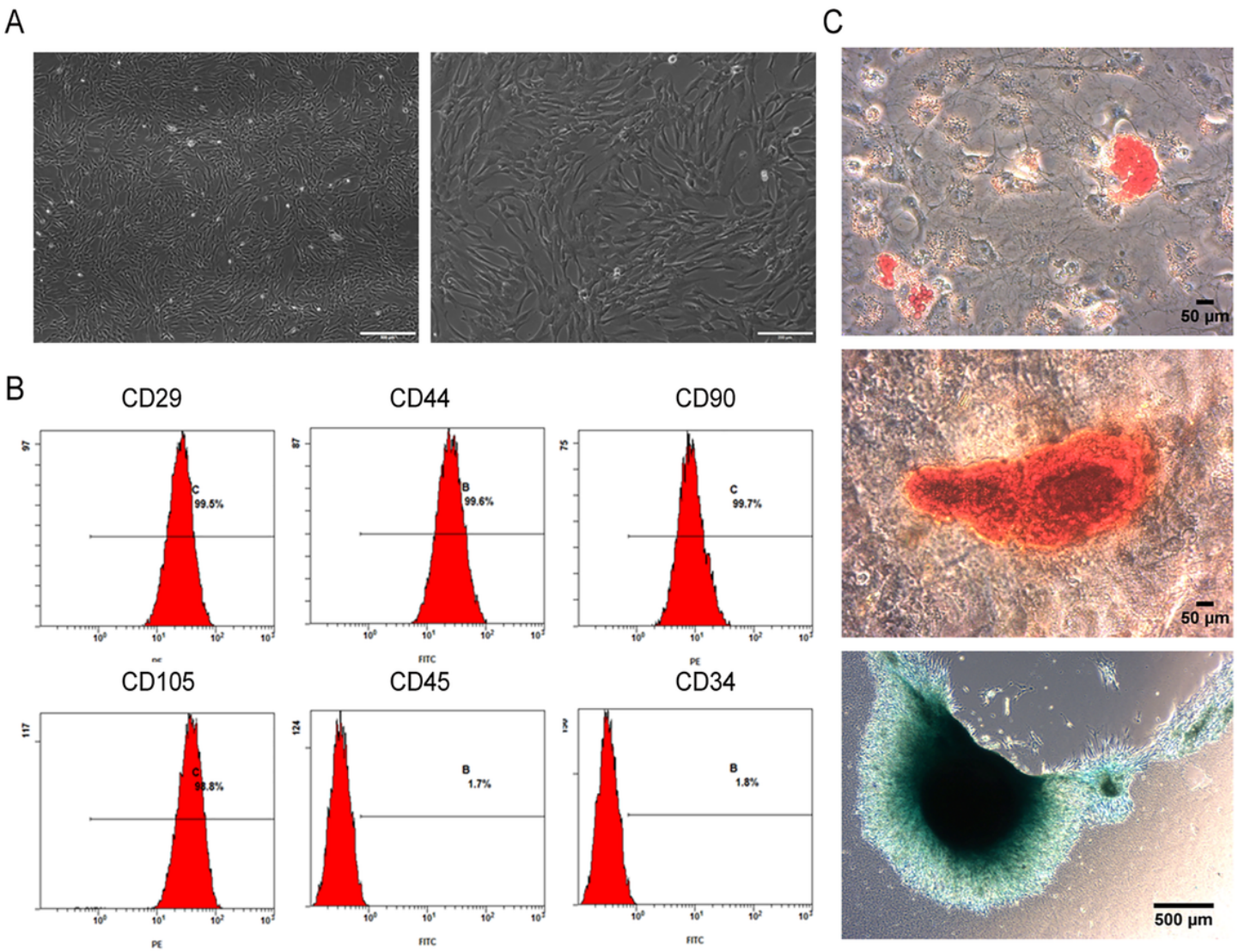

Figure 1

Characterization of hUCMSCs. (A) HUCMSCs exhibited fibroblast-like morphology. Scale bar, 500 μm and 200μm. (B) Flow cytometry analysis of CD29, CD90, CD44, CD105, CD34 and CD45expression in hUCMSCs. (C) Differentiation of hUCMSCs into adipocytes (top row). Scale bar, 50μm, Osteocytes (middle row). Scale bar, 50μm, Chondrocytes (bottom row). Scale bar, 500μm.

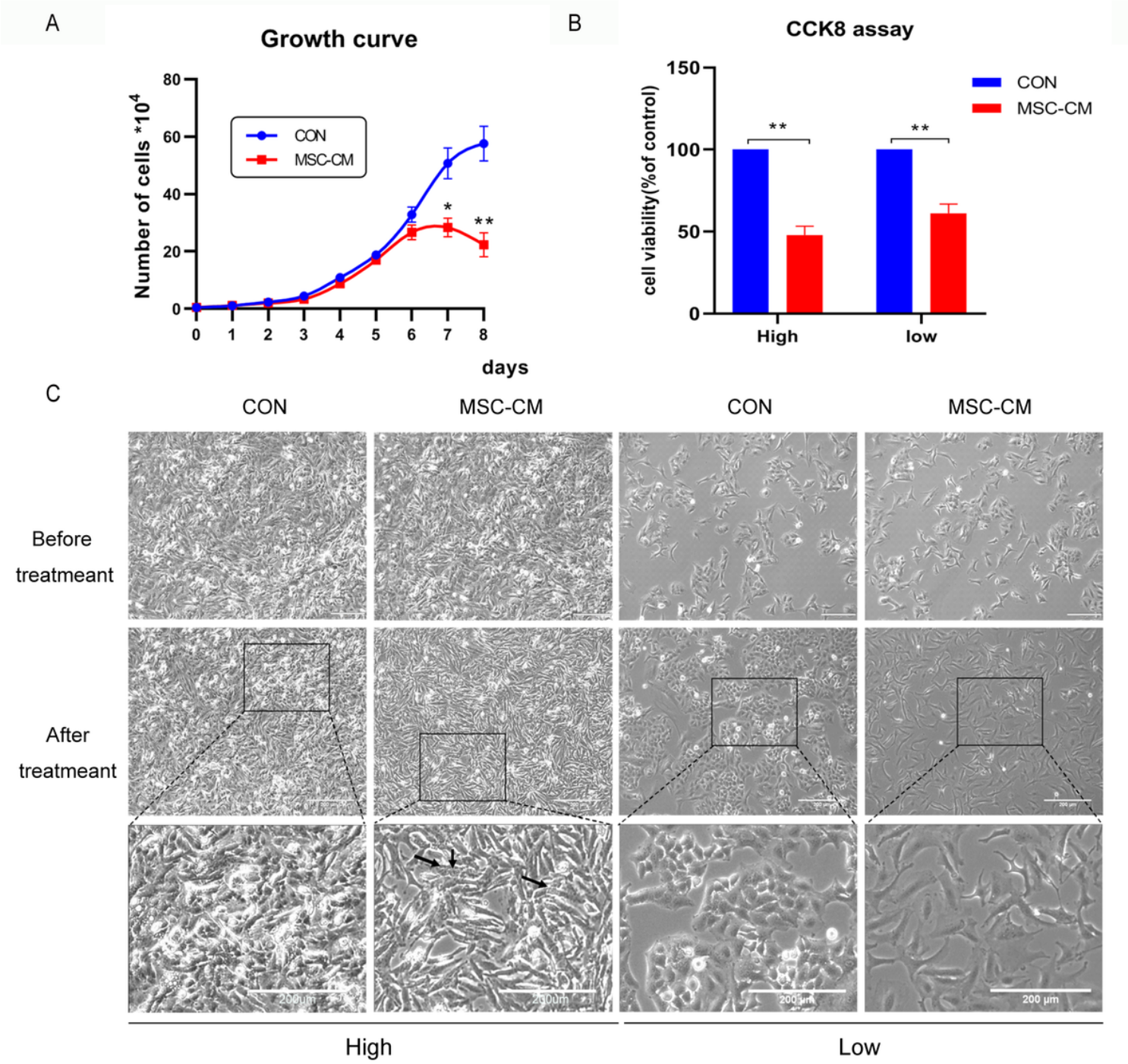

Figure 2

Effect of UCMSCs-CM on proliferation and cell viability of KGN cells. KGN cells were implanted at high (High) and low (Low) density. (A) Growth curve of KGN cells treated with UCMSCs-CM for 8days. (B) CCK8 assays on KGN cells treated with UCMSCs-CM for 48 h. (C) UCMSCs-CM-induced morphological changes in KGN cells, the black arrows represent dead cells. Scale bar, 200μm. *P <0.05, **P < 0.01.

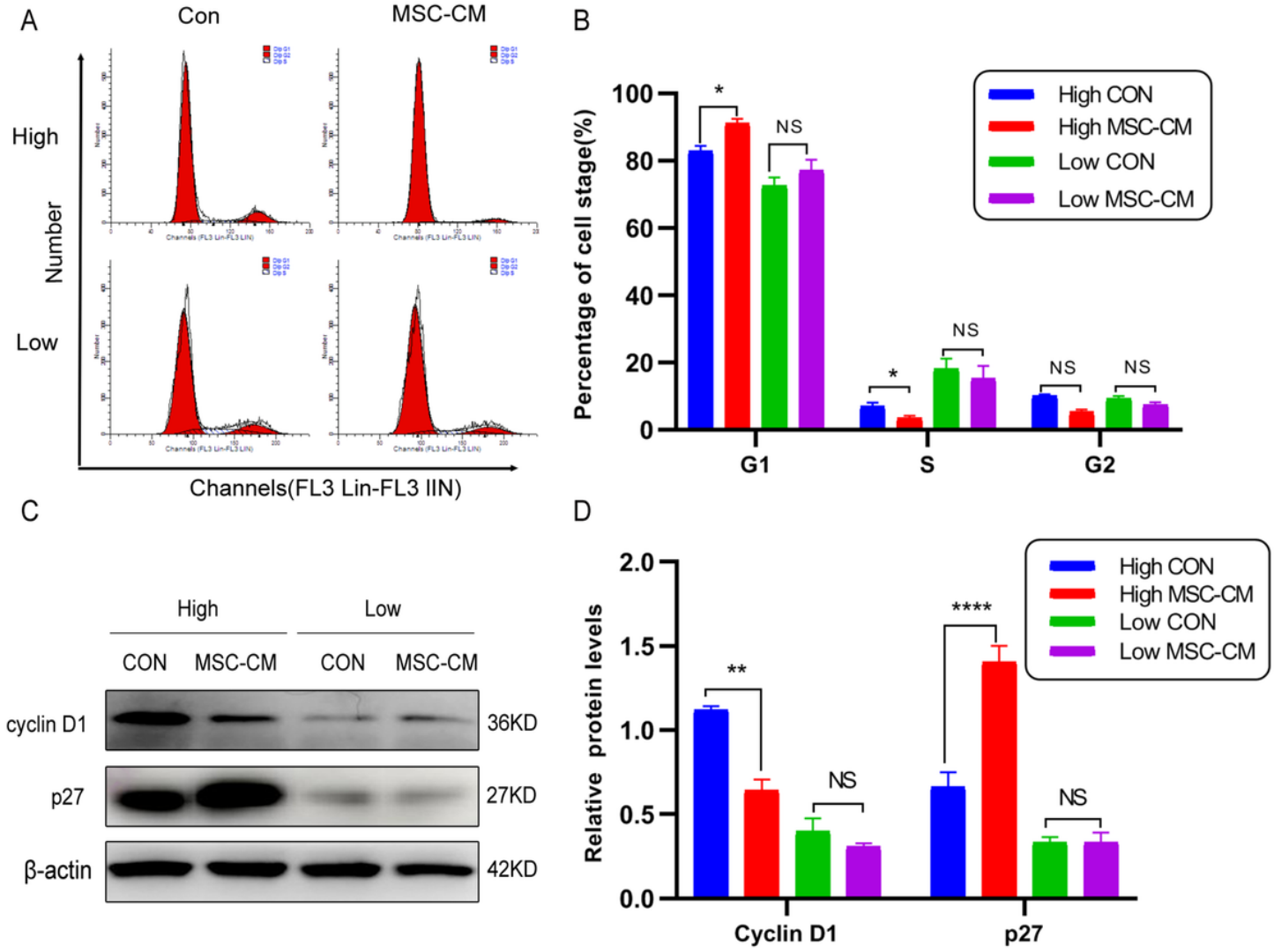

Figure 3

Effect of UCMSCs-CM on cell cycle of KGN cells. KGN cells were implanted at high (High) and low (Low) density. (A) Representative flow cytometry images of KGN cells treated with UCMSCs-CM for 48 h. (B) The quantitative results of flow cytometry assay. (C) The expression of cyclin D1 and p27 in KGNs detected by western blotting. (D) The quantitative results showing the relative expression levels of cyclin D1and P27 proteins. β-actin was used as loading control. *P < 0.05, **P <0 .01, ****P <0 .0001. NS, no statistical difference.

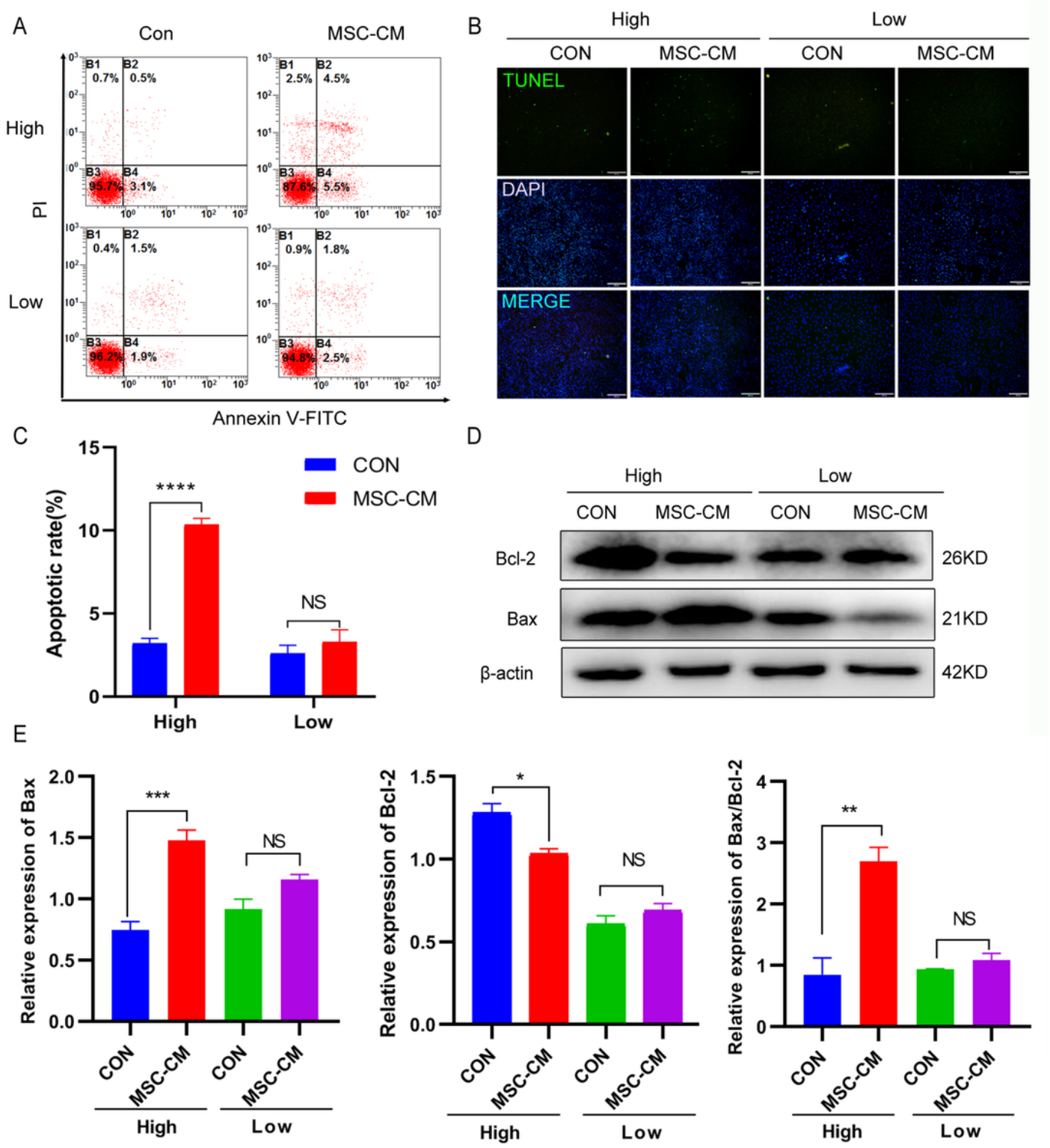

Figure 4

Effect of UCMSCs-CM on apoptosis of KGN cells. KGN cells were implanted at high (High) and low (Low) density. (A) Flow cytometric analysis of apoptosis in KGN cells treated with UCMSCs-CM for 48 h. (B) Representative TUNEL stain images of KGN cells subjected to UCMSCs-CM treatment. Scale bar, 200μm. (C) The quantitative results of flow cytometry assay. (D) Expression of Bax and Bcl-2 measured by western blot. (E) The quantitative results showing the relative expression levels of Bax and Bcl-2 proteins

and the ratio of Bax/Bcl-2. β-actin was used as loading control. *P < 0.05, **P < 0.01, ***P < 0.001, ****P < 0.0001. NS, no statistical difference.

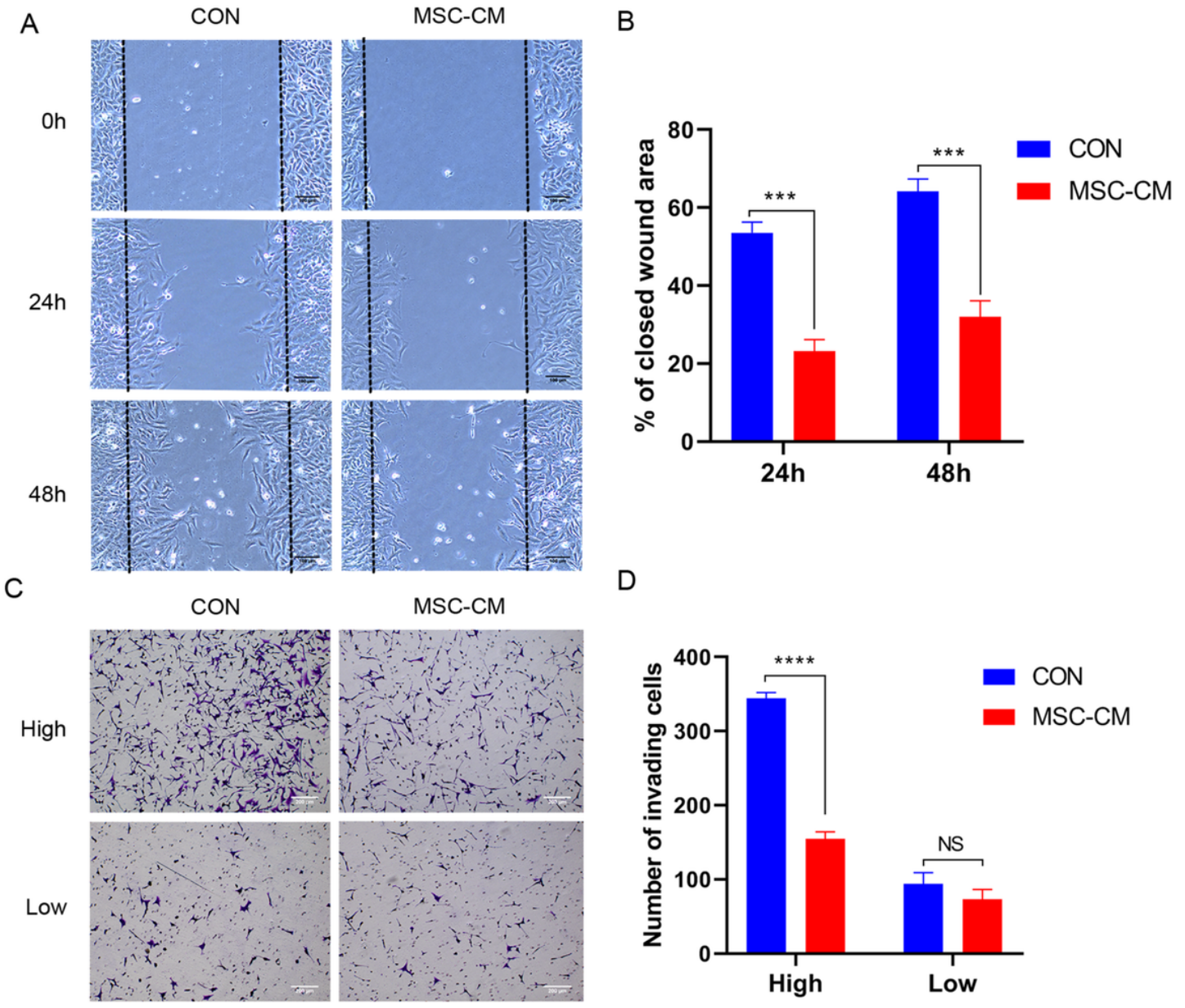

Figure 5

Efect of UCMSCs-CM on migration and invasion of KGN cells. KGN cells were implanted at high (High) and low (Low) density. (A) Scratch wound assays of KGN cells treated with UCMSCs-CM for 24 h and 48h. Scale bar, 200μm. (B) Quantification of the closed wound area for KGN cells. (C) Representative images of invasion assays. Scale bar, 200μm. (D) The quantitative results of invading cell numbers. ***P < 0.001, ****P < 0.0001. NS, no statistical difference.

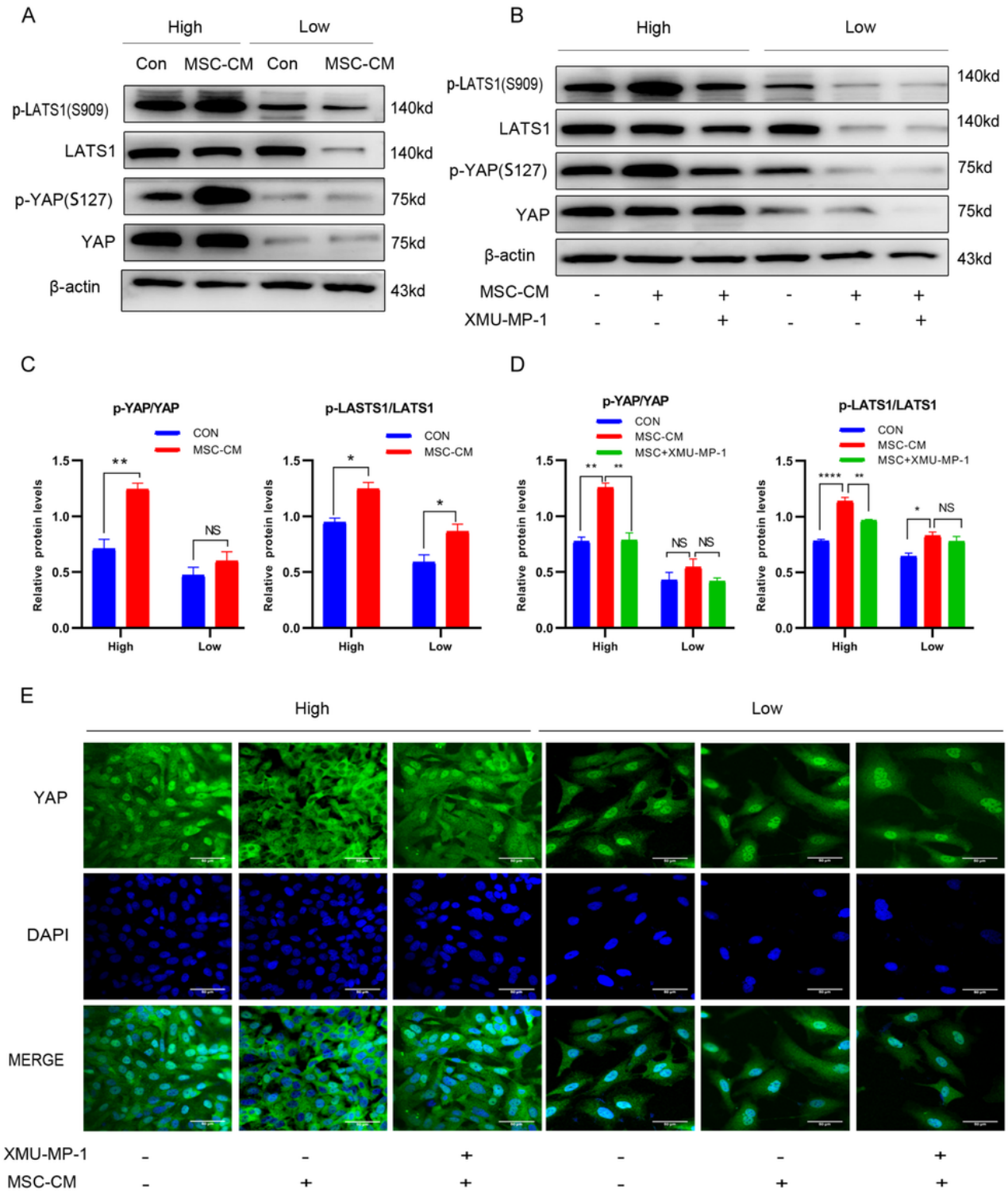

Figure 6

UCMSCs-CM activated the Hippo signaling in KGN cells at high density. KGN cells were implanted at high (High) and low (Low) density. (A) Expression of p-LAST1 (S909), LAST1, p-YAP (ser127), and YAP detected by western blot analysis. (B) KGNs pretreated with XMU-MP-1 and cultured with UCMSCs-CM treatment for 48 h. Expression of p-LAST1 (S909), LAST1, p-YAP (ser127), and YAP detected by western blot analysis. (C-D) The quantitative results showing the ratio of p-LAST1/ LAST1 and p-YAP

(ser127)/YAP. (E) Representative immunofluorescence images of KGN cells stained with anti-YAP (green), DAPI (blue). Scale bar, 50μm. β -actin was used as loading control.*P < 0.05, **P < 0.01, ****P < 0.0001. NS, no statistical difference.

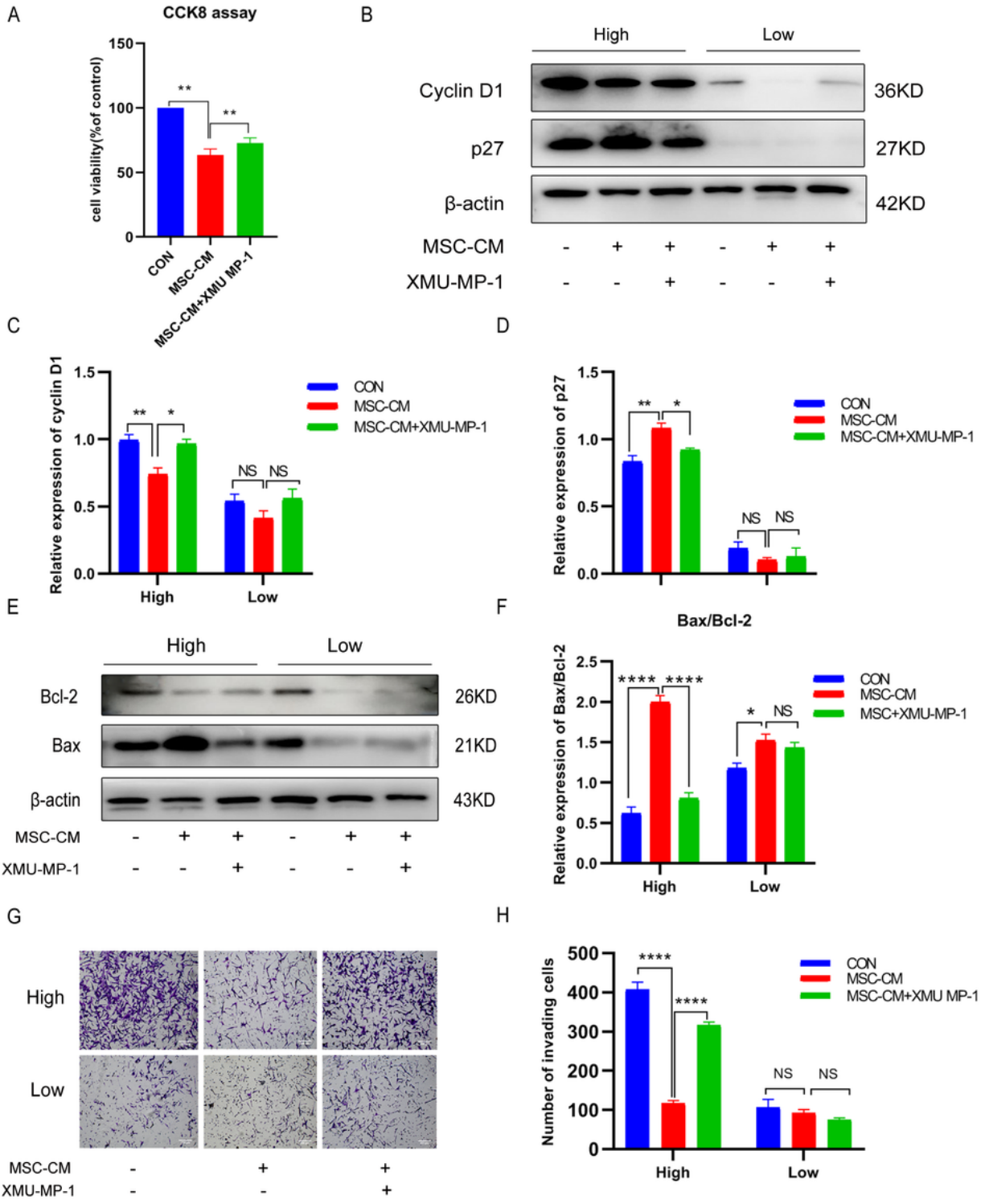

Figure 7

UCMSCs-CM suppresses the malignant phenotype depend on activating the Hippo pathway. KGN cells pretreated with 5μM XMU-MP1 and cultured with UCMSCs-CM for 48 h at high (High) and low (Low) density. (A) The cell viability was examined by CCK-8 assay. (B) Expression of Cyclin D1 and p27 detected by western blot. (C) The quantitative results showing the relative expression levels of Cyclin D1. (D) The quantitative results showing the relative expression levels of p27. (E) Expression of Bax and Bcl-2 detected by western blot. (F) The quantitative results showing the ratio of Bax / Bcl-2. (G) Representative images of invasion assays. Scale bar, 200μm. (H) The quantitative results of invading cell numbers. *P < 0.05, **P < 0.01, ****P < 0.0001. NS, no statistical difference.

Supplementary Files

This is a list of supplementary files associated with this preprint. Click to download.

- graphicabstract.tif